

**AD-A256 819**



AEROSPACE REPORT NO.  
TR-0091(6935-06)-4

(2)

## Some Observations on Stress Graphitization in Carbon-Carbon Composites

Prepared by

R. J. ZALDIVAR and G. S. RELICK  
Mechanics and Materials Technology Center  
Technology Operations

**S** DTIC  
ELECTE  
NOV 06 1992  
**A** **D**

15 September 1992

Prepared for

SPACE AND MISSILE SYSTEMS CENTER  
AIR FORCE MATERIEL COMMAND  
Los Angeles Air Force Base  
P. O. Box 92960  
Los Angeles, CA 90009-2960

Engineering and Technology Group

**92-28869**



THE AEROSPACE CORPORATION  
El Segundo, California

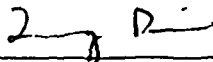
APPROVED FOR PUBLIC RELEASE;  
DISTRIBUTION UNLIMITED

92 11 03 005

This report was submitted by The Aerospace Corporation, El Segundo, CA 90245-4691, under Contract No. F04701-88-C-0089 with the Space and Missile Systems Center, P.O. Box 92960, Los Angeles, CA 90009-2960. It was reviewed and approved for The Aerospace Corporation by R. W. Fillers, Principal Director, Mechanics and Materials Technology Center. P. M. Propp was the project officer for the Mission-Oriented Investigation and Experimentation (MOIE) program.

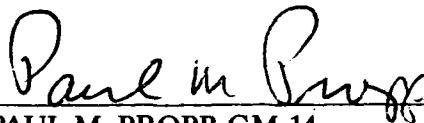
This report has been reviewed by the Public Affairs Office (PAS) and is releasable to the National Technical Information Service (NTIS). At NTIS, it will be available to the general public, including foreign nationals.

This technical report has been reviewed and is approved for publication. Publication of this report does not constitute Air Force approval of the report's findings or conclusions. It is published only for the exchange and stimulation of ideas.



---

QUANG BUI, Lt, USAF  
MOIE Project Manager



---

PAUL M. PROPP, GM-14  
Wright Laboratory, West Coast Office

UNCLASSIFIED

SECURITY CLASSIFICATION OF THIS PAGE

## REPORT DOCUMENTATION PAGE

1a. REPORT SECURITY CLASSIFICATION <b>UNCLASSIFIED</b>			1b. RESTRICTIVE MARKINGS		
2a. SECURITY CLASSIFICATION AUTHORITY			3. DISTRIBUTION/AVAILABILITY OF REPORT		
2b. DECLASSIFICATION/DOWNGRADING SCHEDULE			Approved for public release; distribution unlimited.		
4. PERFORMING ORGANIZATION REPORT NUMBER(S)  TR-0091(6935-06)-4			5. MONITORING ORGANIZATION REPORT NUMBER(S)  SSD-TR-92-23		
6a. NAME OF PERFORMING ORGANIZATION  Technology Operations		6b. OFFICE SYMBOL (If applicable)		7a. NAME OF MONITORING ORGANIZATION  Space and Missile Systems Center	
6c. ADDRESS (City, State, and ZIP Code) The Aerospace Corporation El Segundo, CA 90245-4691			7b. ADDRESS (City, State, and ZIP Code) Los Angeles Air Force Base Los Angeles, CA 90009-2960		
8a. NAME OF FUNDING/SPONSORING ORGANIZATION		8b. OFFICE SYMBOL (If applicable)		9. PROCUREMENT INSTRUMENT IDENTIFICATION NUMBER  F04701-88-C-0089	
8c. ADDRESS (City, State, and ZIP Code)			10. SOURCE OF FUNDING NUMBERS		
			PROGRAM ELEMENT NO.	PROJECT NO.	TASK NO.
			WORK UNIT ACCESSION NO.		
11. TITLE (Include Security Classification)  Some Observations on Stress Graphitization in Carbon-Carbon Composites					
12. PERSONAL AUTHOR(S)  Zaldivar, Rafael J., and Rellick, Gerald S.					
13a. TYPE OF REPORT		13b. TIME COVERED FROM _____ TO _____		14. DATE OF REPORT (Year, Month, Day) 1992 September 15	
				15. PAGE COUNT 36	
16. SUPPLEMENTARY NOTATION					
17. COSATI CODES			18. SUBJECT TERMS (Continue on reverse if necessary and identify by block number)		
FIELD	GROUP	SUB-GROUP	Graphitization		
			Carbon-carbon composites		
			Orientation		
			Carbon fibers		
19. ABSTRACT (Continue on reverse if necessary and identify by block number) The <i>in situ</i> stress graphitization behavior of hard carbons in unidirectionally aligned carbon-carbon (C/C) composites was studied for three carbon fibers (PAN-based T-50, pitch-based PX7, and rayon-based WCA) and two carbon precursor resins [phenol-formaldehyde (SC1008), and polyarylacetylene (PAA), a high-char-yielding, low-shrinkage resin]. Graphitization was followed by measurements of density, transverse thermal expansion, d-spacing by x-ray diffraction (XRD), and by scanning electron microscopy (SEM). In conjunction with xenon-ion etching, the SEM technique was found to be particularly effective in identifying localized regions of graphitized matrix. Results reveal that the graphitization of the composite is significantly greater than graphitization of fiber or matrix alone to the same temperatures. SEM observations indicate that graphitization is confined to the matrix, usually as a sheathlike structure adjacent to the fiber and 1-3 $\mu$ m thick. Such localized graphitization, usually termed stress graphitization, is believed to be the result of thermally induced tensile or compressive stresses acting at the fiber-matrix interface. Debonded regions, which are believed to either initiate at heatup or grow from preexisting cracks in the resin-matrix composite, show less stress graphitization than well-bonded regions, presumably because the debond gaps impede stress buildup at the fiber-matrix interface.					
20. DISTRIBUTION/AVAILABILITY OF ABSTRACT  <input type="checkbox"/> UNCLASSIFIED/UNLIMITED <input checked="" type="checkbox"/> SAME AS RPT. <input type="checkbox"/> DTIC USERS			21. ABSTRACT SECURITY CLASSIFICATION  Unclassified		
22a. NAME OF RESPONSIBLE INDIVIDUAL			22b. TELEPHONE (Include Area Code)		22c. OFFICE SYMBOL

19. ABSTRACT (Continued)

Studies with three different fibers and one matrix (PAA) in matrix-rich composites showed variable degrees of localized stress graphitization, suggesting that the thermal expansion stresses responsible for stress graphitization vary with different fiber-matrix combinations. One consequence of a well-oriented stress-graphitized sheath was found to be debonding of fiber and matrix. Possible reasons for such debonding are discussed briefly.

## PREFACE

We express sincere appreciation to our colleagues at Aerospace: Mr. Jim Noblet and Mr. Joe Uht for their technical assistance; Dr. Gary Steckel and Dr. Dick Chang for valuable comments and suggestions in their reviews of the manuscript; Dr. Chang also for his instructive tutorials on composite mechanics; and Dr. Rokuro Muki for translating a number of articles from Japanese. We thank Mr. Julius Jortner of Jortner Research and Engineering for many useful discussions and for calling our attention to various references. We also thank Dr. Jim Zimmer of Acurex Corp. and Dr. Dennis Nagle of Martin Marietta Research Laboratories for helpful suggestions. One of us (RJZ) wishes to thank The Aerospace Corporation for financial support in the form of a Corporate Fellowship.

This report was first published in the journal *Carbon* 29(8), 1155 (1991).

Accession For	
NTIS CRA&I	<input checked="checked" type="checkbox"/>
DTIC TAB	<input type="checkbox"/>
Unannounced	<input type="checkbox"/>
Justification	
By	
Distribution/	
Availability Codes	
Dist	Avail' and/or Special
A-1	



## CONTENTS

PREFACE .....	1
I. INTRODUCTION .....	7
II. EXPERIMENTAL .....	11
III. RESULTS AND DISCUSSION .....	13
A. Density Measurements .....	13
B. X-Ray Diffraction .....	14
C. Thermal Expansion Measurements .....	16
D. Microstructural Characterization .....	18
REFERENCES .....	29





## FIGURES

1.	Measured density of bulk PAA-derived carbon and T-50 fiber at different heat-treatment temperatures .....	13
2.	Measured and calculated densities of T-50/PAA composites versus heat-treatment temperature .....	14
3.	X-ray diffraction profile of bulk PAA-derived carbon heat-treated to 2750°C .....	15
4.	(002) diffraction peaks of T-50/PAA carbon-carbon composites heat-treated to various temperatures .....	16
5.	Transverse coefficient of thermal expansion (CTE) versus heat-treatment temperature for T-50/PAA carbon-carbon composites .....	17
6.	SEM micrograph of bulk PAA-derived carbon heat-treated to 2700°C .....	18
7.	SEM and optical micrographs of PAA-derived carbon-carbon composites heat-treated to various temperatures .....	19
8.	SEM micrograph of the evolution of microstructure in PAA-derived C/C composites heat-treated for 1 hr at 2500°C and 2800°C .....	22
9.	SEM micrographs showing the debonded microstructures of a phenolic-derived composite and the well-bonded microstructure of PAA-derived composites .....	23
10.	(002) diffraction plots of PAA/T-50 and phenolic/T-50 carbon-carbon composites heat-treated to 2400°C and 2750°C .....	25
11.	SEM micrographs of various filaments embedded in PAA-derived carbon matrix heat-treated to 2750°C .....	27

## TABLE

1.	Properties of Carbon Fibers Used .....	11
----	--	----



## I. INTRODUCTION

The graphitization behavior of hard carbons has become a matter of technological importance because of the widespread use of thermosetting resins as the precursor to the matrix phase in carbon-carbon (C/C) composites. As a general rule, soft, or graphitizing, carbons are derived from asphaltic precursors such as coal-tar and petroleum pitches. These materials are unique in passing through a liquid-crystalline, mesophase state prior to carbonization. In contrast, hard, or nongraphitizing, carbons are usually obtained from thermosetting resins, which do not fuse on pyrolysis but, rather, char in place. It is now well established that, in order to obtain significant graphitization in hard carbons, external stress must be applied at some point in the heat-treatment process.

Franklin, in a now-classic paper [1], was the first to note the importance of internal stresses in the graphitization process. She observed that, in addition to the diffuse (002) band in some hard carbons heat-treated to 2160°C, there were one or two fine lines corresponding to a highly graphitic phase. From the position of the fine (002) line, she calculated a d-spacing of 3.36 Å. Such a d-spacing is obtained in graphitizing carbons only after heat treating to ~ 3000°C. This enhanced graphitization was explained by Franklin as being the result of large compressive stresses set up within the material, owing to restrained thermal expansion of the highly crosslinked system.

Franklin's simple model was one of very small carbon crystallites having thermal expansivities very close to that of single-crystal graphite, but strongly interconnected through a system of crosslinks that restrict the volume expansivity of the bulk material to about 1/7th that of the single-crystal value. She postulated that, when some of the crosslinks break randomly, the freed crystallites are subjected to very high compressive forces, resulting in the observed enhanced graphitization.

Since Franklin's early observations, there have been numerous experiments on graphitization of hard carbons under mechanical load. Much of the work dealing with the application of hydrostatic pressure during heat treatment has been done by Noda and coworkers and is reviewed by Noda [2]. Briefly, they found that pressures of 0.1 to 1 GPa (1–10 kbar) had a dramatic accelerating effect on the graphitization of both soft and hard carbons. For example, Kamiya *et al.* [3], using hydrostatic pressures of 0.5 GPa with a hard carbon derived from phenol-formaldehyde resin, found that nearly complete graphitization could be achieved for a heat-treatment time of 60 min at 1500°C. Interestingly, graphitization began at a lower temperature and, for a given temperature, proceeded more extensively in the hard carbon than in a graphitizing polyvinylchloride coke. This difference has been explained by Fischbach [4] as being the result of the addition of the external stress and high internal stresses in the hard carbons. In the soft carbons, the internal stresses are believed to be much lower.

The idea of the additivity of stresses has been exploited by various workers in pulverized glassy carbon or binder-filler composite systems. For example, Chard *et al.* [5] heat-treated a pulverized low-temperature (1000°C) glassy carbon to 2650°C at pressures from 46 to 90 MPa

(6700 to 13,000 psi). From metallographic examinations, they observed that contact between angular particles was often associated with areas of intense optical anisotropy. Those same areas, when observed by scanning electron microscopy (SEM) following ion-bombardment etching, revealed pronounced lamellar features that were taken as evidence of graphitic structure. The lamellae were normal to the apparent direction of local compressive stress as deduced from the geometry of the contact areas, suggesting to those authors that compressive stress promotes basal-plane alignment normal to the stress. It was interesting that a glassy carbon heat-treated to 3000°C did not reveal any evidence of graphitic structure, suggesting that the 3000°C heat treatment "stabilized" the structure against graphitization.

Reiswig *et al.* [6] did a similar investigation of a composite with a polyfurfuryl alcohol (PFA) binder and pulverized glassy carbon filler derived from PFA. PFA is typically nongraphitizing. They found extensive optical anisotropy in the PFA binder by 900°C; lamellae formation was observed by SEM, in the range 2000–2200°C; and extensive graphitization ( $d_{002} = 0.336$  nm) was observed at 2700°C. That both filler and binder were derived from PFA, and only the binder was graphitized, suggests that internal stresses generated during matrix shrinkage facilitate graphitization. Similar results were obtained by Cornault *et al.* [7], using composites of furfuryl alcohol resin with various carbon and graphite fillers.

Korosonov *et al.* [8] extended this research a step further and studied the graphitization behavior of a series of phenol-furfural-formaldehyde resins by applying a mechanical load of 19.7 MPa (2860 psi) over selected temperature ranges. They found that when the mechanical load was applied over the 400–600°C range, subsequent heat treatment of the resin-derived carbon to 2800°C resulted in pronounced graphitic character [ $d_{002} = 0.337$  nm, crystallite thickness ( $L_c$ ) = 35 nm]. However, when this same load was applied consecutively from 20 to 400°C and from 600 to 2300°C, the carbon structure was glassy ( $d_{002} = 0.342$  nm,  $L_c < 5$  nm). With no application of load, the structure was even more disordered ( $d_{002} = 0.345$  nm,  $L_c < 5$  nm). Their results strongly suggested that a stress-induced ordering effect, occurring when the material is most deformable [9], is the principal factor in predisposing the carbon to graphitization during subsequent high-temperature heat treatment.

Kimura *et al.* [10] obtained similar results by hot-pressing specimens of furfuryl alcohol resin and then heat-treating to 3000°C. They found that when a pressure of only 2 MPa (290 psi) was applied from room temperature (RT) to 2100°C, the resulting d-spacing was 0.336 nm; when a pressure of 18 MPa (2600 psi) was applied over the range 400–1000°C, the d-spacing was 0.335 nm. When this same 18 MPa was applied from RT to 400°C, and in a second specimen from 1000 to 2100°C, the resulting d-spacings were 0.342 and 0.344 nm, respectively. However, in neither of these two studies do the authors report the fraction of resin that transformed to the graphitic structure. It appears that their results could be explained by the transformation of only a small fraction of material.

Kamiya and Suzuki [11], in a very interesting series of experiments, studied the structure of phenol-formaldehyde resin chars heat-treated to 2700°C. They observed that concentric layers of graphitic carbon formed around the periphery of pores. They then removed the

graphitic regions by wet oxidation and subsequently heat-treated the specimens to 2700°C. They found no indication of further graphitization, suggesting once again that the precursor to the graphitic regions was formed in the carbonization stage.

Hishiyama *et al.* [12] were the first to report detailed characterization of the graphitization behavior of a hard-carbon matrix in a *continuous-fiber-reinforced* unidirectional C/C composite. They used commercial polyacrylonitrile (PAN)-based carbon fibers with a furfuryl alcohol resin binder. X-ray diffraction (XRD), SEM, density, and magnetoresistance were consistent in showing enhanced matrix graphitization with heat-treatment temperatures (HTTs) to 2000°C. More specifically, they observed that the apparently anisotropic regions began at the interface and grew into the matrix. They first observed the formation of optical anisotropy at an HTT of 1000°C, concluding that the large shrinkage stresses of the matrix on carbonization were probably the principal factor in orientation development and subsequent graphitizability. However, as pointed out by Inagaki *et al.* [13], whether such regions of optical anisotropy are due to internal stresses or to real anisotropic texture is still an open question. The work in graphitization of soft and hard carbons through 1967 is well reviewed by Fischbach [4].

We present here some observations of the graphitization behavior of combinations of two hard-carbon matrices and three fibers within unidirectional C/C composites. Emphasized particularly is the role of fiber-matrix interfacial stress and its variation with fiber, matrix, and processing temperature, in promoting stress graphitization.



## II. EXPERIMENTAL

The principal fiber used in this study was T-50 PAN-based carbon fiber from Amoco (3000 filaments/bundle). Amoco's PX7 pitch-based carbon fibers and their rayon-based WCA fibers (removed from fabric) were also used. Properties of the different fibers used are given in Table 1.

Table 1. Properties of Carbon Fibers Used

Fiber (Amoco)	Precursor	Tensile Modulus (GPa)	Density (g/cm <sup>3</sup> )
PX7	Pitch	896 (130 Mpsi)	2.20
T-50	PAN	379 (55 Mpsi)	1.80
WCA	Rayon	34 (~5 Mpsi)	1.40

The principal matrix-precursor resin was polyarylacetylene (PAA), which is a high-temperature thermoset resin synthesized from meta- and para-diethynylbenzene. The first step in the synthesis of PAA is a nickel-catalyzed cyclotrimerization reaction that creates a low molecular weight prepolymer, which is dissolved in methylethylketone (MEK). The attraction of PAA as a C/C matrix precursor is its high char yield (~90%) and good processability [14]. The chemistry of PAA is discussed by Barry *et al.* [15]. In the present work, the T-50 carbon fiber bundles were impregnated with a solution of PAA in MEK. The MEK was evaporated in air, leaving the PAA polymer impregnated in the fiber bundles. The preimpregnated fiber bundles were then stacked into a mold and cured under pressure.

A phenolic resin was also used in this study. It was purchased from the Borden Corporation and is designated SC1008. Unidirectional composites made from this resin by the above method were first carbonized to 1200°C in a nitrogen atmosphere. After carbonization, selected samples of both composite systems were heat-treated in an induction-heated graphitization furnace at 1800, 2400, and 2750°C for 1 hr in a flowing argon atmosphere.

Specimens were analyzed by XRD using a computer-controlled vertical powder diffractometer equipped with a graphite crystal monochromator and a scintillation detector. The bulk PAA samples, after various heat treatments, were ground to -250 to +350 mesh powders. The composite specimens were run as solids; they were polished to 2 mils (0.005 mm) thickness and had planar dimensions of 0.5 x 0.5 in. (12.7 x 12.7 mm). The graphite (002) reflection was scanned from 22° to 29° at a speed of 2.4°/min, with operating conditions of 45 kV and 38 mA.

A Dupont 1090 thermo-mechanical analyzer (TMA) was used to measure the transverse coefficient of thermal expansion of T-50/PAA C/C composites. Specimen dimensions were 5 x 5 x 12 mm. The measurement was conducted under a nitrogen atmosphere, and each cycle consisted of a ramp from 25 to 700°C/min and back down to 25°C. Five cycles were run for each sample.

Optical and scanning electron microscopy were used to examine the evolution of microstructure after various heat treatments. All SEM specimens were xenon-ion-etched to enhance the textural distinction between glassy and graphitic-type carbon [5,6]. Measurements of real density were obtained by mercury intrusion porosimetry.



### III. RESULTS AND DISCUSSION

#### A. DENSITY MEASUREMENTS

Figures 1 and 2 show plots of room-temperature density versus heat-treatment temperature for bulk PAA, T-50 fibers, and T-50/PAA C/C composites. The two PAA systems have identical cure, postcure, and final heat-treatment schedules. The measured real density of the T-50 fibers was  $1.80 \pm 0.05 \text{ g/cm}^3$  for all HTTs, which agrees with Amoco's reported data. For *bulk* PAA (Fig. 1) there is an increase in density from 1.1 to  $1.55 \text{ g/cm}^3$  from the cured state to the end of carbonization ( $1200^\circ\text{C}$ ). In the range  $1200\text{--}2300^\circ\text{C}$ , there is a slight decrease in density around  $1800^\circ\text{C}$  followed by an increase to a stable value of about  $1.65 \text{ g/cm}^3$  at  $2450^\circ\text{C}$  and above. Similar trends in density versus HTT were reported by Kipling *et al.* [16] for a series of nongraphitizable carbons. They explained the density decrease as the result of the formation of closed microporosity. The very low density is an indication of the nongraphitizability of PAA carbon in *bulk form*.

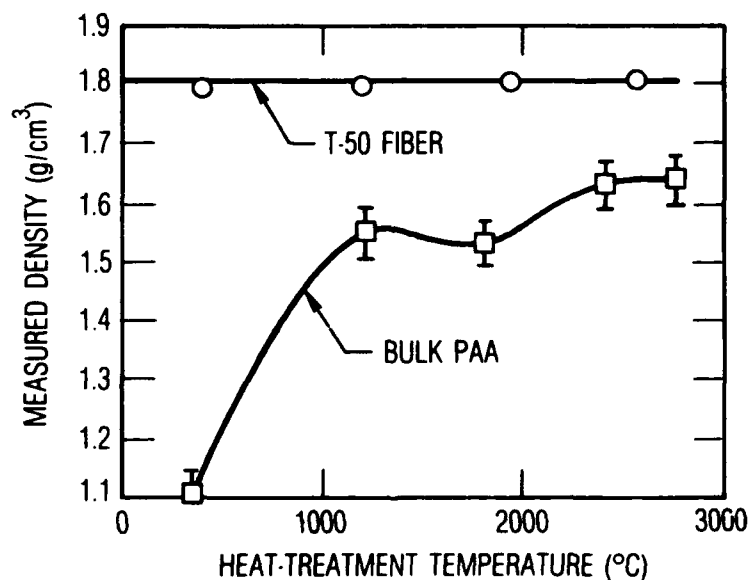


Figure 1. Measured density of bulk PAA-derived carbon and T-50 fiber at different heat-treatment temperatures.

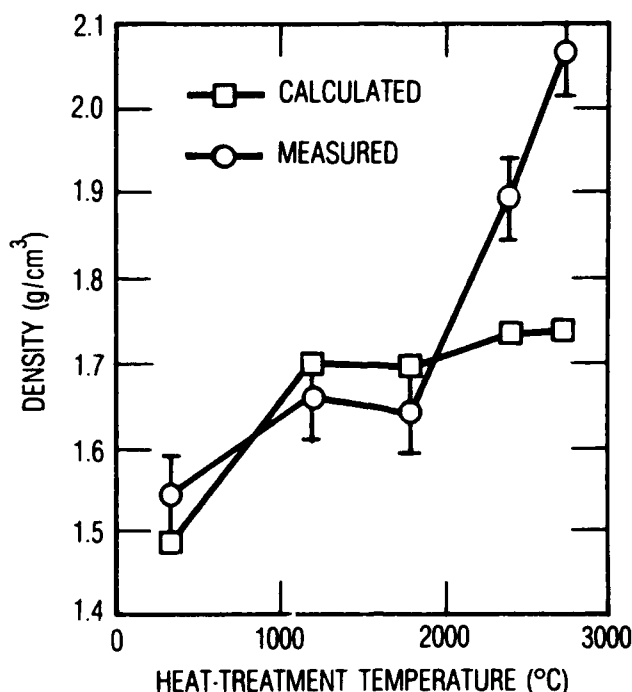


Figure 2. Measured and calculated densities of T-50/PAA composites versus heat-treatment temperature.

If the *in situ* matrix density is the same as the bulk matrix density at all temperatures, and the density of fiber remains constant (at 1.80 g/cm<sup>3</sup>), then the density of the composites can be calculated from rule-of-mixtures if the volume fractions of fibers, matrix, and porosity are also known. The volume fractions of fiber and matrix for these composites were obtained by taking a series of SEM micrographs and measuring the respective cross-sectional areas. Mercury porosimetry was used to measure the porosity at each HTT. The calculated and measured densities for the C/C composites heat-treated at various temperatures are plotted in Fig. 2. The much larger measured composite density above 2300°C indicates that the fiber and/or matrix experiences some degree of *in situ* graphitization at the higher HTTs.

## B. X-RAY DIFFRACTION

Figure 3 shows an XRD profile of PAA-derived carbon heat-treated in bulk form to 2750°C. The broad peak is the (002) reflection corresponding to a d-spacing of ~0.35 nm. From the Scherrer equation [4], the crystallite thickness  $L_c$  of the system is calculated to be of the order of only 2.0 nm.

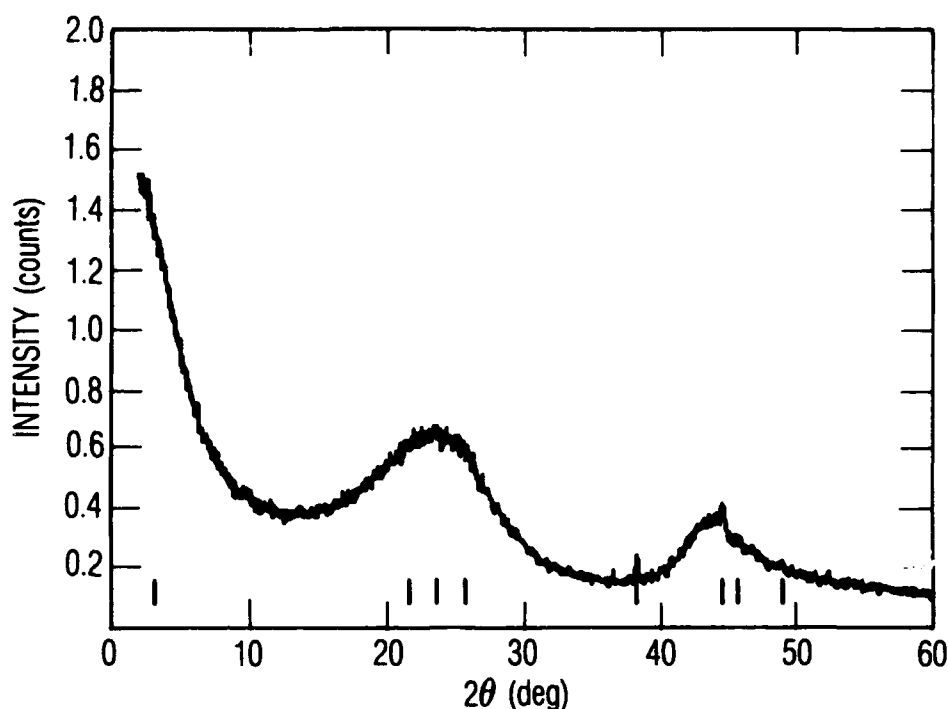


Figure 3. X-ray diffraction profile of bulk PAA-derived carbon heat-treated to 2750°C.

The (002) diffraction peaks for the T-50/PAA C/C composite heat-treated to various temperatures are shown in Fig. 4. These scans were obtained by projecting the x-ray beam such that only those layer planes parallel to the fiber axis were in the diffraction condition. For an HTT of 1200°C, the (002) peak is very broad and symmetrical about  $2\theta = 26^\circ$  ( $d_{002} = 0.343$  nm) and is almost totally the diffraction response of the fiber as determined from XRD on bare fibers heated to 1200°C. For 1800°C, the peak remains centered about the same  $2\theta$  value but shows some narrowing. For 2400°C, the curve becomes asymmetrical, suggesting the presence of a second curve convoluted with the fiber curve. At 2750°C, the curve develops a well-defined shoulder on the high angle side of the peak; the shoulder corresponds closely to the characteristic d-spacing for single-crystal graphite.

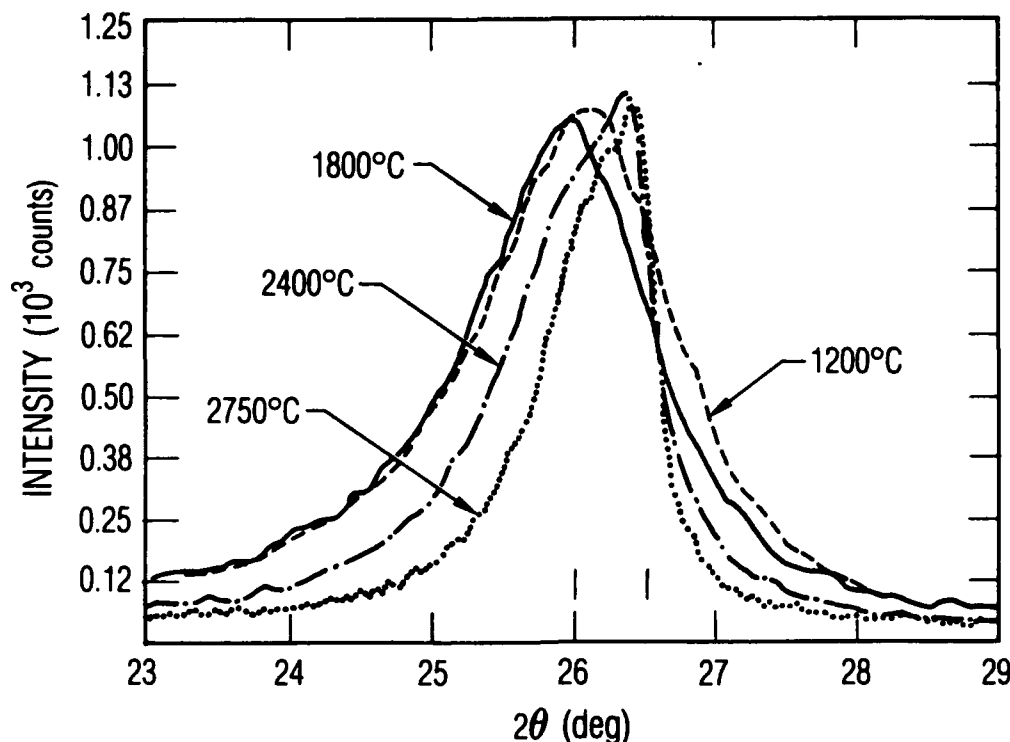


Figure 4. (002) diffraction peaks of T-50/PAA carbon-carbon composites heat-treated to various temperatures.

It is very unlikely that the crystalline peak has any significant contribution from the fiber. Johnson [17] showed that hot-stretching at 2800°C, and elongations of nearly 30%, were necessary to increase the modulus of PAN-based carbon fibers from 60 to 90 Mpsi. From this observation, we infer that the fiber structure remained essentially that of an oriented glassy carbon. And more relevant to the current study, recent transmission electron microscopy (TEM) studies by Kowbel *et al.* [18] of a PAN-based 3-D C/C composite heated repeatedly to temperatures in the vicinity of 2700°C revealed no significant enhancement in fiber structure. The crystalline peak, therefore, is taken to be evidence of *in situ matrix* graphitization.

### C. THERMAL EXPANSION MEASUREMENTS

The development of graphitization and preferred orientation in unidirectional composites can also be followed by thermal expansion measurements. The transverse coefficient of thermal expansion (CTE) of T-50/PAA unidirectional composites versus HTT is shown in Fig. 5. Each CTE point is the average of five secant-slope measurements over the range 25–750°C. Following an initial rise in CTE between HTTs of 1200 and 1600°C, owing to an increase in

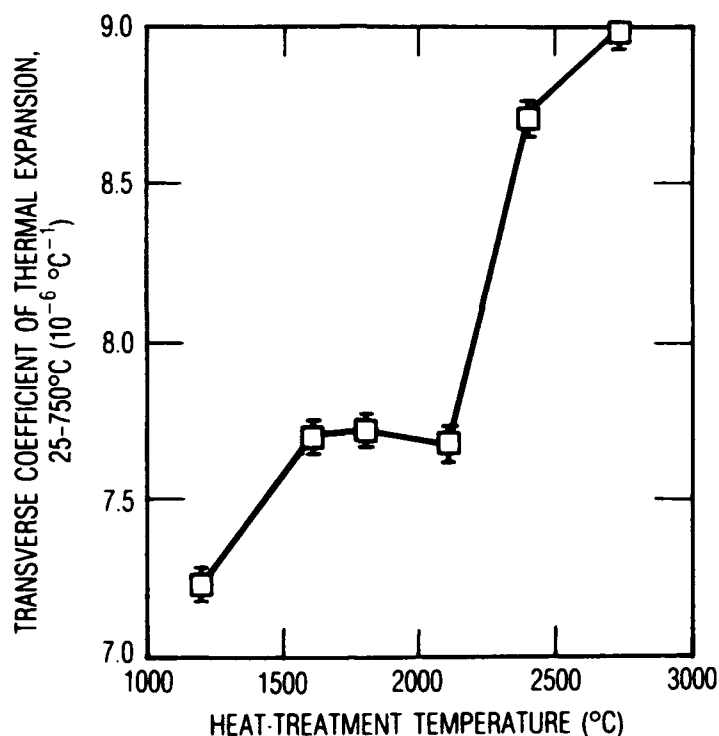


Figure 5. Transverse coefficient of thermal expansion (CTE) versus heat-treatment temperature for T-50/PAA carbon-carbon composites. Each CTE point is the average of 5 cycles from 25 to 750°C.

fiber volume fraction, the transverse CTE remains constant between HTTs of 1600 and 2100°C. However, above 2100°C there is a large increase in transverse CTE, which is consistent with an increase in preferred orientation of the matrix parallel to the fiber surfaces. This abrupt point of transition in transverse CTE appears to be a sensitive indicator of the critical temperature of onset of matrix graphitization.

To determine whether this increased CTE may have been due to an increase in preferred orientation of the fiber, a T-50/PAA composite was fabricated with fibers that had been heat-treated to 2800°C to stabilize the graphitization and orientation of the fiber against subsequent reheatings. It was found that the transverse CTE of composites fabricated with these pretreated fibers had the same behavior as that shown in Fig. 5, indicating that the effect was due to matrix orientation.

#### D. MICROSTRUCTURAL CHARACTERIZATION

Figure 6 shows an SEM of PAA-derived carbon heat-treated *in bulk* to 2700°C. Figures 7a–d show PAA-derived carbon in unidirectional composites heat-treated to 1800, 2100, 2400, and 2750°C; the photos on the left are polarized-light micrographs and those on the right are SEMs. Xenon-ion etching was employed to bring out the distinction between graphitic and nongraphitic carbon, as mentioned above.

The appearance of lamellar texture is consistent with the presence of graphitelike layer planes oriented perpendicular to the plane of section, i.e., parallel to the fiber axes. Such texture is brought about by differential etching rates of different microstructural units, the exact nature of which is still unclear. The most likely mechanism seems to be preferential removal at lower density, less-ordered intercrystalline-type boundaries that separate regions of good crystalline registry [19]. This effect is seen very dramatically in pyrolytic graphites reacted in oxygen [20,21]. However, the technique of ion bombardment using chemically unreactive species has the advantage of more localized and better controlled etching because of the absence of any exothermic effects. These figures clearly illustrate the difference between the isotropic nature of PAA when heated in bulk form and the more crystalline carbon matrix that results in the composite. The polarized-light micrographs show the increasing optical anisotropy that accompanies increasing graphitization.

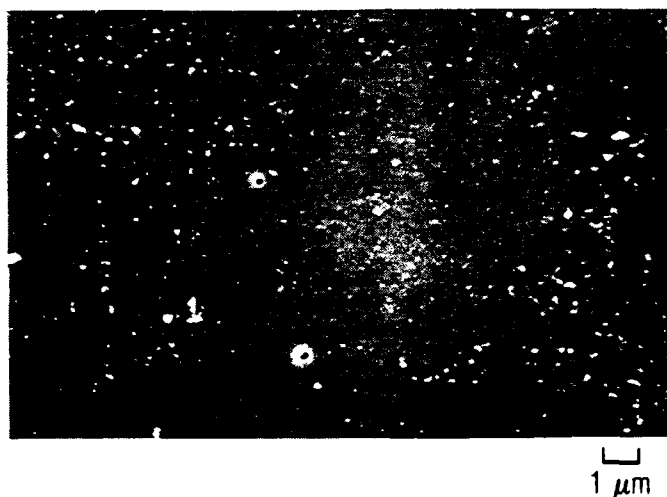


Figure 6. SEM micrograph of bulk PAA-derived carbon heat-treated to 2700°C.

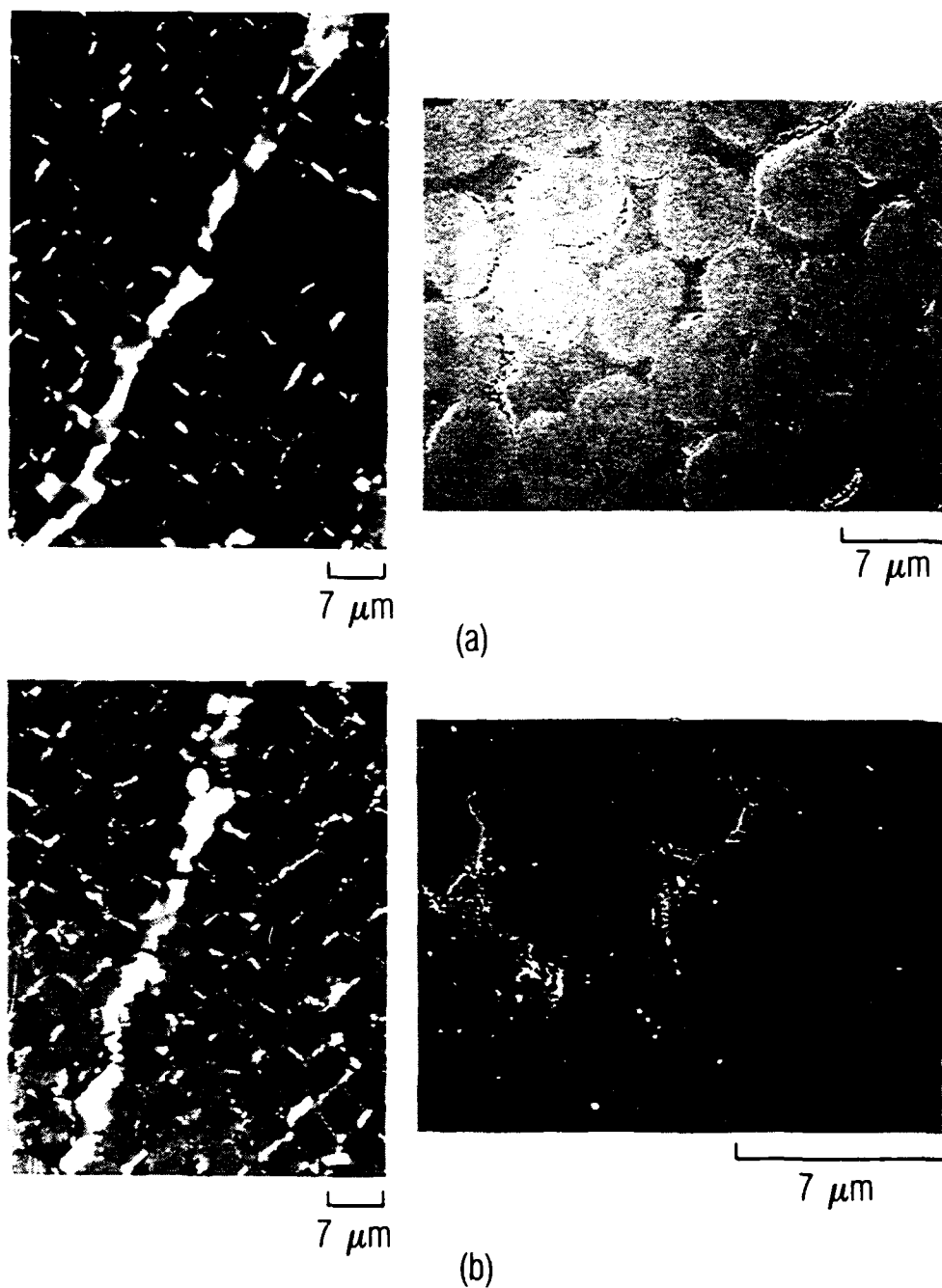


Figure 7. SEM (right side) and optical (left side) micrographs of PAA-derived carbon-carbon composites heat-treated to various temperatures: (a) 1800°C, (b) 2100°C, (c) 2400°C, (d) 2750°C.

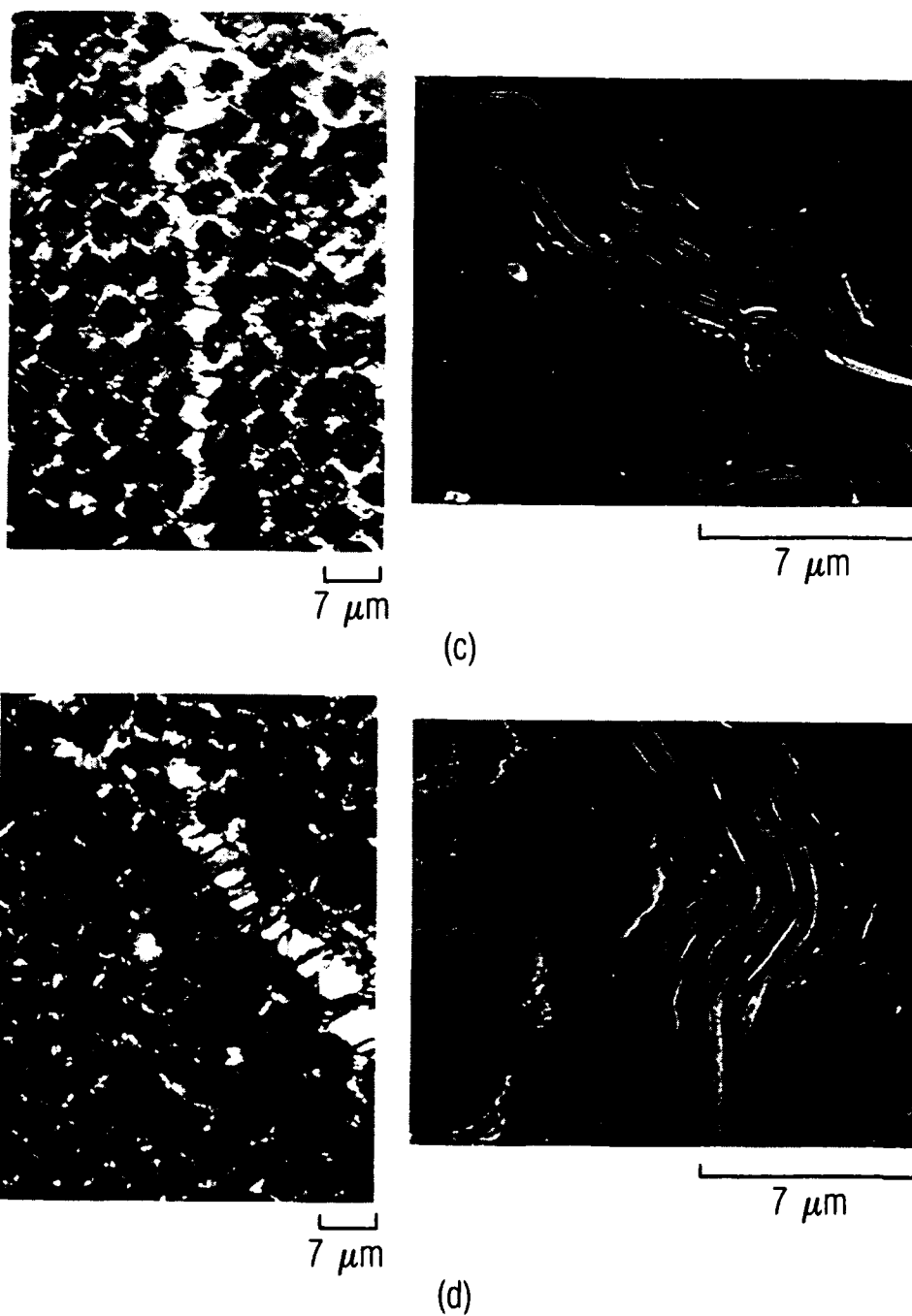


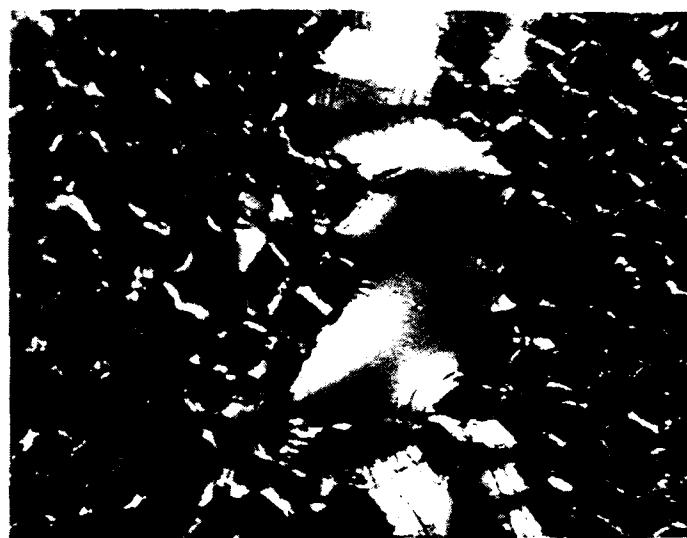
Figure 7 (Cont'd). SEM (right side) and optical (left side) micrographs of PAA-derived carbon-carbon composites heat-treated to various temperatures: (a) 1800°C, (b) 2100°C, (c) 2400°C, (d) 2750°C.



Figures 8a-b are micrographs taken under cross-polarized light of ion-etched specimens heat-treated at 2500°C and 2800°C, respectively, for approximately 1 hr. The use of ion-etching in conjunction with polarized-light microscopy reveals the lamellar texture and optical activity simultaneously. The pattern of light and dark lines corresponding to the lamellar regions is probably the result of two factors: the first is that the etching has produced a pattern of hills and valleys, with resulting differential light scattering between the two; the second is that the etching has enlarged these "defective" regions so that they are now resolvable by optical microscopy.

These photos are evidence that the optical activity seen in these materials is a result of anisotropic structure. If the brighter regions were due to stress alone, we would not see the pattern of 0°/90° extinction contours, and we would expect graphitized regions to be less bright owing to stress relaxation associated with graphitization. That this is not the case is seen clearly in Figs. 8a-b. Figure 8b is very interesting in that it reveals what appear to be well-defined crystallographic tilt boundaries in the stress-graphitized matrix. Figure 8b also shows that despite the extensive graphitization in this region, areas of glassy-carbon-type structure are still evident.

Figures 9a-b present, for direct comparison, SEM micrographs of phenolic and PAA-derived unidirectional composites reinforced with T-50 fibers and heat-treated to 2400°C (following carbonization to 1200°C). Both photos show matrix-rich areas within a multi-tow unidirectional composite. These areas are similar to those found at yarn crossover sites in 2-D and 3-D C/C composites. The matrix in the phenolic-derived composite completely debonds and, at the same time, remains amorphous in the matrix-rich area. In contrast, the PAA-derived composite has remained well bonded throughout and shows large lamellar regions indicative of graphitic structure.



(a)

7  $\mu\text{m}$



(b)

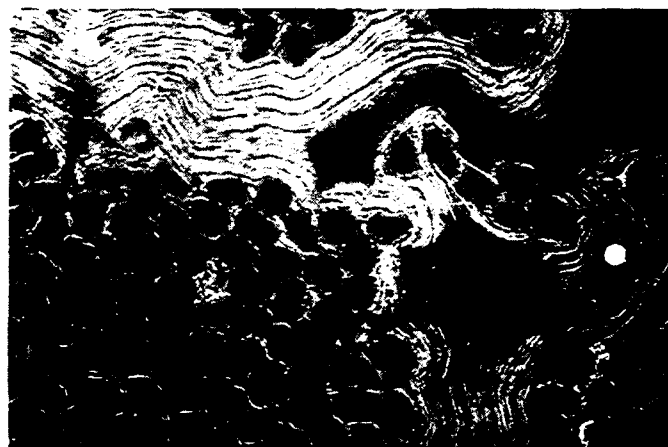
20  $\mu\text{m}$

Figure 8. SEM micrograph of the evolution of microstructure in PAA-derived C/C composites heat-treated for 1 hr at (a) 2500°C and (b) 2800°C.



(a)

10  $\mu\text{m}$



(b)

7  $\mu\text{m}$

**Figure 9.** SEM micrographs showing (a) the debonded microstructure of a phenolic-derived composite and (b) the well-bonded microstructure of PAA-derived composites. Both heated to 2400°C. Note the lamellar microstructure developed in the PAA carbon.

The debonding in the phenolic system appears to be clearly tensile. Given a simple model of a single filament embedded in a block of resin matrix, we would expect radial stresses to be compressive at the fiber-matrix interface during pyrolysis because of the large net shrinkage of the pyrolyzing resin. (Linear shrinkage to 750°C for phenolic and PAA resins is approximately 20% and 6%, respectively [14].) Associated with such radial compressive stress is a circumferential tensile stress in the matrix. By this model, and assuming the composite stays bonded, radial tensile stresses could develop at some point on cooldown if there was significant compressive stress relaxation due to creep; this then would be a possible explanation for the observed matrix debonding.

However, Jortner [22] has pointed out that the size of the debond gaps usually is much too large to be explained by thermal contraction strains only. He also showed [23], by hot-stage microscopy observations of 2-D carbon-fiber/resin laminates undergoing pyrolysis to carbon-carbon, that cracks existing in the cured resin system open on heatup during pyrolysis. Very few new cracks were seen to form. From measurements of relative displacements from the hot-stage micrographs, Jortner has shown that the strain fields during pyrolysis are very complex. Therefore, it seems reasonable to conclude that the matrix debond in Fig. 9a occurred prior to or early in the pyrolysis. It follows, then, that, in the phenolic-derived composite, there is a temperature range over which crack closure must first occur, owing to differential thermal expansion between fiber and matrix. This situation must occur before interface compressive and tensile stresses can begin to develop. Over that temperature range, the debonded matrix behaves as *unreinforced bulk* material heat-treated to the same temperatures, i.e., without stress acting on it. Therefore, we would expect higher stresses in the resin-rich areas of the T-50/PAA system at any given temperature. The greater degree of debonding in the phenolic resin system may be a result of its larger pyrolysis shrinkage.

In contrast to resin-rich areas, matrix-lean regions reflect more accurately the environment typically encountered within individual fiber bundles. In the matrix-lean areas, for both PAA and phenolic matrix systems, the fiber and matrix are observed to remain well bonded through the heatup and cooldown cycles. Figure 10 shows the (002) x-ray diffraction plots of PAA- and phenolic-derived T-50 C/C single-tow composites heat-treated to 2400 and 2750°C for 1 hr. The PAA- and phenolic-resin-derived composites have comparable fiber volumes; so, nominally, the scans reflect differences in matrix crystallinity. In contrast to the SEM photos of resin-rich areas (Fig. 9), which show the PAA-derived matrix to be better graphitized, the XRD results on the whole composite suggest that the two matrices have comparable crystal-line development at 2400 and 2750°C (d-spacings of both are approximately 3.37 Å, indicating a high degree of graphitization relative to these matrices heat-treated in bulk form).

The possibility that there may be some contribution from the fiber cannot be discounted totally; confirmation or denial of this will require more detailed experimental studies. Nevertheless, the results suggest that differences in stress graphitization between PAA- and phenolic-derived carbons is significant only in resin-rich areas where the greater debonding in the phenolic system, possibly caused by larger pyrolysis shrinkage stresses, impedes the buildup of interface stresses. In more typical, matrix-lean regions, the higher shrinkage of the phenolic resin may be a factor in promoting stress graphitization.

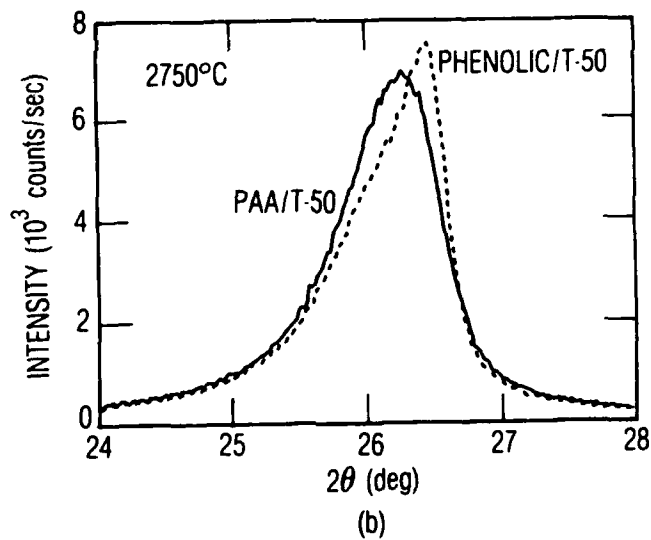
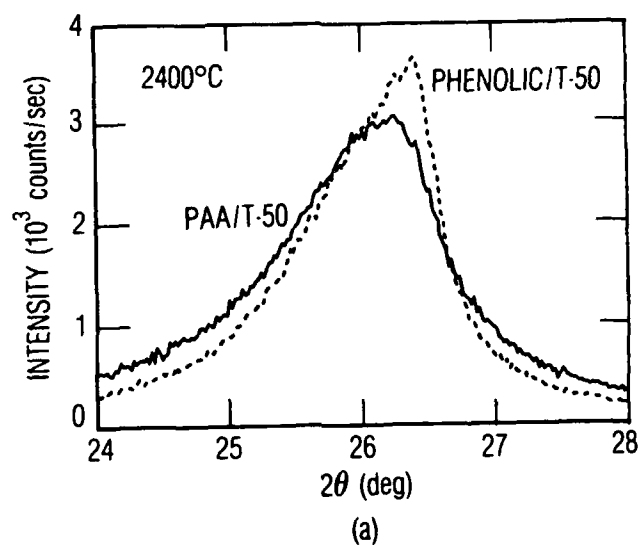


Figure 10. (002) diffraction plots of PAA/T-50 and phenolic/T-50 carbon-carbon composites heat-treated to (a) 2400°C and (b) 2750°C.

To better assess the different factors involved in stress graphitization, three different fibers (Table 1) were incorporated into a PAA-derived matrix at low fiber volume fraction. The resulting composites were heat-treated to 2750°C, and the stress graphitization behavior was observed by SEM. Since the matrix volume fraction in these composite specimens is very high, the stresses at the isolated fiber-matrix interfaces during pyrolysis and subsequent heating are probably uniformly compressive. The results for the PX7 fibers, shown in Fig. 11a, are a well-aligned graphitic sheath around the fibers and debonding of the sheath from the fiber. Over 95% of the filaments in this sample were completely debonded, leaving the pronounced sheath structure seen in the figure.

In the T-50 composites, three types of sheath structure were observed. In Fig. 11b the sheath exhibits a very well-ordered lamellar structure, 2-3  $\mu\text{m}$  thick, which is completely debonded from the fiber. Figure 11c shows an almost totally debonded T-50 filament with a less-oriented sheath structure; and Fig. 11d shows a very well-bonded T-50 filament and a smaller, more diffuse type of matrix sheath.

Figure 11e is a representative view of a rayon-based WCA carbon filament inside a PAA-derived carbon matrix. In all cases the WCA filaments remained bonded to the matrix after heat treatment and cooldown, and the sheath was not well oriented.

The development of a graphitic matrix sheath is clearly a factor in controlling the debonding within the composite fiber bundles; in turn, debonding affects the load-transfer capability at the fiber-matrix interface. Excluding regions of large pyrolysis debonds, such as those in Fig. 9a, we observe that in the composites that form a well-graphitized sheath, the fiber becomes debonded from the matrix. On the other hand, if a well-ordered sheath does not develop, it is likely that the filaments and matrix would stay well bonded.

These bonding/debonding phenomena also involve a number of other factors. The first is the volume decrease associated with graphitization of the matrix sheath. Second, the more graphitic the matrix sheath is, the fewer are the edge-type carbon atoms to remain attached and bonded to the adjacent fiber and the lower is the interfacial bond strength to resist tensile debonding. Third, the well-ordered matrix sheath would be expected to have lower transverse strength and higher thermal expansion, so that on cooling, transverse failure of the matrix sheath could also occur much more readily. That is, there would be decreased strength of both fiber-matrix interface and the stress-graphitized matrix sheath. A fourth factor is stress relaxation. As graphitization proceeds with a net decrease in volume of matrix, the effect is to reduce the compressive stresses at the interface. This stress reduction would be particularly important if stress graphitization were a high-temperature phenomenon since the graphitization would then be self-limiting. On the other hand, if the oriented precursor structure of the graphitic sheath is formed during pyrolysis, as suggested [6-8,10-12], and is unaffected by the stresses generated at graphitization temperatures, then the stress relaxation would be relatively unimportant.

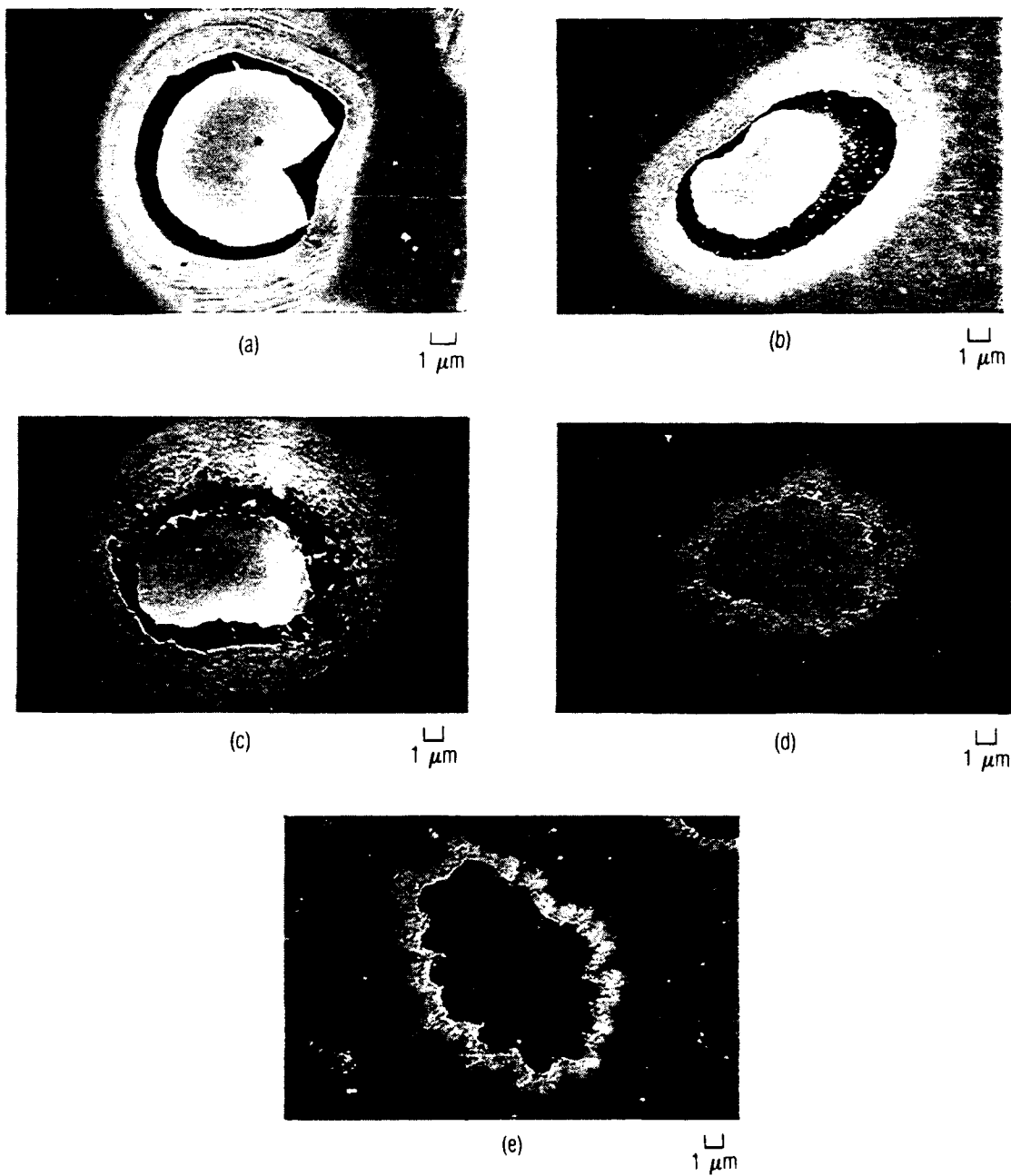


**Figure 11. SEM micrographs of various filaments embedded in PAA-derived carbon matrix heat-treated to 2750°C: (a) PX7; (b), (c), and (d) T-50; and (e) WCA.**

From a practical standpoint, since the mechanical properties of C/C composites can be strongly influenced by the structure of the matrix immediately adjacent to the fiber, in designing C/Cs, it is of great importance to take into account the matrix stress graphitization that may result from interface stresses generated by different fiber, matrix, and processing combinations.



## REFERENCES

1. R. E. Franklin, *Proc. R. Soc. London, Ser. A* **A209**, 196 (1951).
2. T. Noda, *Carbon* **6**, 125 (1968).
3. K. Kamiya, M. Inagaki, M. Mizutani, and T. Noda, *Bull. Chem. Soc. Jpn.* **41**, 2169 (1968).
4. D. B. Fischbach, "Kinetics and Mechanisms of Graphitization," In *Chemistry and Physics of Carbon* (Edited by P. L. Walker, Jr.), Vol. 7, pp. 1-105, Marcel Dekker, NY (1971).
5. W. C. Chard, R. D. Reiswig, L. S. Levinson, and T. D. Baker, *Carbon* **6**, 950 (1968).
6. R. D. Reiswig, L. S. Levinson, and J. A. O'Rourke, *Carbon* **6**, 124 (1968).
7. P. Cornault, F. Du Chaffant, I. Rappeneau, M. Yvars, and A. Fillatre, *Carbon* **6**, 857 (1968).
8. A. Korosonov, A. Vinnikov, V. I. Frolov, and B. G. Ostronov, *Dok. Akad. Nauk SSSR* **185**, 1316 (1969).
9. F. Fitzner and A. Burger, In *Carbon Fibers: Their Composites and Applications*, paper 36, p. 134, The Plastics Institute, London (1971).
10. S. Kimura, Y. Tanabe, and E. Yasuda, In *Proc. Fourth Japan-U.S. Conf. Compos. Mater.*, p. 867, Washington, DC (1988).
11. K. Kamiya and K. Suzuki, *Carbon* **13**, 317 (1975).
12. Y. Hishiyama, M. Inagaki, S. Kimura, and S. Yamada, *Carbon* **12**, 249 (1974).
13. M. Inagaki, A. Oberlin, and S. de Fonton, *High Temp.-High Press.* **9**, 453 (1977).
14. G. Binegar, J. Noblet, R. Zaldivar, P. Sheaffer, and G. S. Rellick, *Effects of Heat Treatment on Microstructure and Flexural Properties of Unidirectional Carbon-Carbon Composites*, Report No. TR-0089(4935-06)-2, The Aerospace Corp., El Segundo, CA (1 November 1989).
15. W. T. Barry, C. Gaulin, and R. Kobayashi, *Review of Polyarylacetylene Matrices for Thin-Walled Composites*, Report No. TR-0089(4935-06)-1, The Aerospace Corp., El Segundo, CA (25 September 1989).
16. J. J. Kipling, J. N. Sherwood, P. V. Shooter, and N. R. Thompson, *Carbon* **1**, 321 (1964).
17. W. Johnson, In *Third Conf. on Indust. Carbons and Graphites*, p. 447, Society of Chemical Industry, London (1971).
18. W. Kowbel, P. S. Chen, and H. Yenchang, *Ultramicroscopy* **29**, 98 (1989).

19. J. M. Thomas, "Microscopic Studies of Graphite Oxidation," In *Chemistry and Physics of Carbon* (Edited by P. L. Walker, Jr.), Vol. 1, pp. 121-202, Dekker, NY (1965).
20. F. Rodriguez-Reinoso and P. A. Thrower, *Carbon* **12**, 269 (1974).
21. G. S. Rellick, P. A. Thrower, and P. L. Walker, Jr., *Carbon* **13**, 71 (1975).
22. J. Jortner, private communication.
23. J. Jortner, "Microstructure of Cloth-Reinforced C-C Laminates," *Carbon* (in press).
24. L. A. Feldman, *High-Temperature Creep of Carbon Yarns and Composites*, Report No. TOR-0086(6728-02)-2, The Aerospace Corp., El Segundo, CA (30 September 1987).
25. G. Sines, Z. Yang, and B. D. Vickers, *Carbon* **27**, 403 (1989).
26. J. Jortner, In *Ext. Abstr., 15th Biennial Conf. Carbon*, p. 278, Philadelphia, PA (1981).

## TECHNOLOGY OPERATIONS

The Aerospace Corporation functions as an "architect-engineer" for national security programs, specializing in advanced military space systems. The Corporation's Technology Operations supports the effective and timely development and operation of national security systems through scientific research and the application of advanced technology. Vital to the success of the Corporation is the technical staff's wide-ranging expertise and its ability to stay abreast of new technological developments and program support issues associated with rapidly evolving space systems. Contributing capabilities are provided by these individual Technology Centers:

**Electronics Technology Center:** Microelectronics, solid-state device physics, VLSI reliability, compound semiconductors, radiation hardening, data storage technologies, infrared detector devices and testing; electro-optics, quantum electronics, solid-state lasers, optical propagation and communications; cw and pulsed chemical laser development, optical resonators, beam control, atmospheric propagation, and laser effects and countermeasures; atomic frequency standards, applied laser spectroscopy, laser chemistry, laser optoelectronics, phase conjugation and coherent imaging, solar cell physics, battery electrochemistry, battery testing and evaluation.

**Mechanics and Materials Technology Center:** Evaluation and characterization of new materials: metals, alloys, ceramics, polymers and their composites, and new forms of carbon; development and analysis of thin films and deposition techniques; nondestructive evaluation, component failure analysis and reliability; fracture mechanics and stress corrosion; development and evaluation of hardened components; analysis and evaluation of materials at cryogenic and elevated temperatures; launch vehicle and reentry fluid mechanics, heat transfer and flight dynamics; chemical and electric propulsion; spacecraft structural mechanics, spacecraft survivability and vulnerability assessment; contamination, thermal and structural control; high temperature thermomechanics, gas kinetics and radiation; lubrication and surface phenomena.

**Space and Environment Technology Center:** Magnetospheric, auroral and cosmic ray physics, wave-particle interactions, magnetospheric plasma waves; atmospheric and ionospheric physics, density and composition of the upper atmosphere, remote sensing using atmospheric radiation; solar physics, infrared astronomy, infrared signature analysis; effects of solar activity, magnetic storms and nuclear explosions on the earth's atmosphere, ionosphere and magnetosphere; effects of electromagnetic and particulate radiations on space systems; space instrumentation; propellant chemistry, chemical dynamics, environmental chemistry, trace detection; atmospheric chemical reactions, atmospheric optics, light scattering, state-specific chemical reactions and radiative signatures of missile plumes, and sensor out-of-field-of-view rejection.